UCRL-JRNL-201698

LAWRENCE
LIVERMORE
NATIONAL
LABORATORY

Multiscale Thermohydrologic Model Analyses of Heterogeneity and Thermal-Loading Factors for a Proposed Nuclear Waste Repository

Lee G. Glascoe, Thomas A. Buscheck, James Gansemer, Yunwei Sun, and Kenrick Lee

January 29, 2004

Submitted for publication in *Nuclear Technology*

Multiscale Thermohydrologic Model Analyses of Heterogeneity and Thermal-Loading Factors for a Proposed Nuclear Waste Repository

Lee G. Glascoe, Thomas A. Buscheck, James Gansemer, Yunwei Sun, and Kenrick Lee

Mailstop L-103, Lawrence Livermore National Laboratory

Livermore, CA 94551

KEYWORDS: Thermal-hydrology, Yucca Mountain, Multiscale Modeling

Biographies

Lee G. Glascoe (BS, civil engineering, University of Washington, 1991; MS, environmental engineering, University of Michigan, Ann Arbor, 1993; MS, mechanical engineering, University of Michigan, Ann Arbor, 1998; PhD, environmental engineering, University of Michigan, Ann Arbor, 1999) is a staff scientist at Lawrence Livermore National Laboratory (LLNL) working on thermohydrology and reactive transport.

Thomas A. Buscheck (BS, civil engineering, Lafayette College, 1976; MS, civil engineering, University of California, Berkeley, 1978; PhD, geological engineering, University of California, Berkeley, 1981) is a senior researcher at LLNL and the task leader of LLNL's Thermohydrologic Modeling Group. He has been working on the Yucca Mountain Project for nearly twenty years.

James Gansemer (BS, industrial engineering, University of Illinois, Champaign, 1990; MS, operations research, University of California, Berkeley, 1991) is a computations expert at LLNL and the developer of the MSTHM process.

Yunwei Sun (BS, hydrogeology, Jilin University, China, 1984; MS, water resources management, Institute of Geography, Chinese Academy of Sciences, 1987; PhD, civil and environmental engineering, Israel Institute of Technology, 1995) is a staff scientist at LLNL and an expert at reactive transport and thermohydrologic modeling.

Kenrick Lee (BS, mining engineering, Queens University, Canada, 1978; MS, mining engineering, New Mexico Technological University, 1985; MS, hydrology, New Mexico Technological University, 1986; PhD, mineral engineering, University of California, Berkeley, 1998) is a senior scientist at LLNL and has worked on both experimental and numerical modeling of thermal and hydrologic processes at Yucca Mountain for over ten years.

ABSTRACT

The MultiScale ThermoHydrologic Model is used to predict thermal-hydrologic conditions in emplacement drifts and the adjoining host-rock throughout a proposed nuclear waste repository. The presented modeling effort simulates a lower temperature operation mode with a different panel loading than the repository currently being considered for the Yucca Mountain license application. Simulations address the influence of repository-scale thermal-conductivity heterogeneity and the influence of pre-closure operational factors on thermal-loading conditions. MSTHM can accommodate a complex repository layout, a development that, along with other improvements, enables more rigorous analyses of pre-closure operational factors. Differences in MSTHM output occurring with these new capabilities are noted for a new sequential waste-package loading technique compared to a standard simultaneous loading technique. Alternative approaches to modeling repository-scale thermal-conductivity heterogeneity in the host-rock units are investigated, and study incorporating geostatistically-varied host-rock thermal conductivity is discussed.

INTRODUCTION

A Brief Overview of MSTHM

The Multi-Scale ThermoHydrologic Model (MSTHM) has been used extensively for the Yucca Mountain Project (1,2,3,4) and addresses multi-scale thermal and hydrologic problems through the use of spatially and sequentially nested numerical submodels. The motivation behind the MSTHM approach is the need for a modeling tool that simultaneously accounts for processes occurring at a scale of a few tens of centimeters around individual waste packages and emplacement drifts, and also at the kilometer-scale of the mountain. At present, a single numerical model cannot account for both of these scales as too large a computational cost is required for performance assessment and engineering design, which necessitate the ability to conduct a large number of realizations. The following description is a brief overview of the MSTHM; a more complete description is found in Buscheck et al. (5,6,7) and BSC (1).

MSTHM captures the three-dimensionality of the site of the proposed Yucca Mountain repository. Stratigraphic variability is consistent with the unsaturated zone hydrology model developed at Lawrence Berkeley Laboratory (8), a nested model that, like MSTHM, simulates both mountain-scale and drift-scale processes. When compared to traditional nested modeling approaches, however, the MSTHM approach is more computationally efficient and is able to resolve greater detail in and around the waste-packages at the drift-scale. MSTHM's use of submodels renders it a particularly efficient and flexible tool for performance confirmation and design as it allows for relative ease of simulation for sensitivity and uncertainty analyses (1). MSTHM has been validated to a three-drift "mini-repository" modeled using a nested one-model approach (5).

The fundamental concept behind MSTHM is a representation of the waste repository through the assembly of several numerical submodels (described in the next subsection), which capture important thermal and hydrologic processes at different spatial scales in a computationally efficient manner. Thermal-hydrology is directly simulated for a line-averaged waste package using a two-dimensional drift-scale cross section for a variety of areal-heat-generation densities and at numerous locations throughout the modeled repository. In these simulations, the flow of liquid and gas through variably saturated fractured porous media is modeled using a dual-permeability description that accounts for two-phase processes such as evaporation, boiling, and condensation (6). The dual-permeability formulation is modeled using the active fracture technique of Liu et al. (9) and fracture-matrix interaction is modeled as a first-order process. While such first-order models have been identified as inaccurate for some problems at early times (10), for the Yucca Mountain Project, the average distance between fracture aperture and the matrix is small thus rendering first-order approximations of fracture-matrix interaction acceptable. The open tunnel drifts are modeled as a porous medium of very high permeability and porosity. The two-dimensional line-averaged submodel represents thermal conduction and convection in rock, and thermal conduction, convection, and radiation in the open cavities in the emplacement drifts. To include three-dimensional mountain-scale processes, the two-dimensional thermal-hydrologic submodel results are interpolated along heating curves obtained from a mountain-scale conduction-only submodel. Temperature and hydrologic variables are then modified with a three-dimensional thermal submodel that accounts for waste-package-to-waste-package variability in heat output (some waste packages generate much less heat than other waste packages). The final result of this assemblage of submodels is the thermal and hydrologic history in and around the drift for any waste-package at any location of the repository.

MSTHM considers the influence of proximity to the edge of the repository, which is important because waste packages close to the repository edge will cool more quickly than ones near the repository center. These repository-edge differences in temperature are assumed to be controlled by thermal conduction in the rock, which is equivalent to saying that convective heat transfer mechanisms have a negligible influence on lateral mountain-scale heat flow. This assumption is based on the findings of Buscheck and Nitao (11) who state that the bulk permeability of the unsaturated zone of Yucca Mountain is much less than the threshold bulk permeability at which buoyant gas-phase convection begins to significantly influence heat flow. However, these convective mechanisms, notably, buoyant gas-phase convection and the heat pipe effect, are included in the two-dimensional thermal-hydrologic submodels of the MSTHM. The assumption of conduction dominance at the mountain scale tends to preserve temperature differences that arise as a result of differences in proximity to the repository edges. The MSTHM approach assumes that any mountain-scale movement of water and water vapor along the drift axes or between drifts can be neglected. MSTHM also neglects any changes in rock properties due to any coupled thermal-hydrologic-chemical-mechanical processes and the effect of dissolved solutes on the thermal-hydrologic properties of water.

The MSTHM represents all possible waste packages emplaced in the repository. The heat-generation-rate-versus-time relationships for the different waste-package types vary and are modeled accordingly. The model effectively considers a narrow range of possible waste-package sequencing that results in eight distinct local heating conditions for waste packages. The specific modeled waste-package types are from hottest to coldest: PWR1-2 (pressurized water reactor type 2), PWR1-1 (pressurized water reactor type 1), BWR1-3 (boiling water reactor), and DHLW (defense high level waste). The MSTHM calculates the following TH variables: temperature, relative humidity, liquid-phase saturation, liquid-phase flux, gas-phase pressure, capillary pressure, water-vapor flux, air flux, and evaporation rate. MSTHM variables are determined at various generic locations in the emplacement drifts and in the near-field host-rock surrounding the drifts.

MSTHM: NUFT Submodels and their Assembly

MSTHM consists of four submodel types, all of which are run using the NUFT computer code (12). These four submodels are the following:

- **SMT** (3-D Smeared-heat-source, Mountain-scale, Thermal-conduction) submodels simulate mountain topographic and stratigraphic effects on repository heating; it models repository panels separately as a smeared heat source and extends ~1km below the water table and ~1km laterally from the repository.

- **LDTH** (2-D Line-averaged-heat-source, Drift-scale, ThermoHydrologic) submodels simulate thermohydrologic processes in the drift and near-field host-rock.

- **SDT** (1-D Smeared-heat-source, Drift-scale Thermal-conduction) submodels tie together the SMT and LDTH submodels.

DDT (3-D Discrete-heat-source, Drift-scale Thermal-conduction-radiation) submodels simulate conduction/radiation/convection heat transfer within the drift thereby capturing waste-package-to-waste-package temperature variability.

For any given MSTHM calculation, LDTH and SDT submodels are run at many geographic locations distributed uniformly over the repository area; these submodels use the stratigraphy, overburden thickness, TH boundary conditions, and percolation fluxes appropriate for each location. At each geographic location, the LDTH- and SDT-submodel calculations are conducted at different values of thermal loading, which can be quantified by an "Areal Mass Loading" (AML), expressed in terms of metric tons of uranium per acre (MTU/acre). Note that MTU, "metric tons of uranium", is the equivalent measure of the mass of radioactive waste and also a measure of thermal power loading (1 MTU=1.323 kW, 1 MTU/acre = 0.327 W/m^2). The *modeled* AML represents the effective heat loading at a specific location and is modeled by varying the drift-spacing within the LDTH- or SDT-submodel of that location. The *emplaced* AML for the repository is obtained by averaging the total repository inventory of 70,000 MTU (93 MW) over the entire heated repository footprint (13). The results from submodels with modeled AMLs less than the emplaced AML account for the evolving influence of the edge-cooling effect, i.e., waste-package locations close to the repository edges cool faster than those at the center. The results from submodels with modeled AMLs higher than the emplaced AML account for waste packages with greater-than-average heat output (see (5) for further details on AML curves).

The LDTH submodel domain is a vertical 2-D drift-scale cross-section, perpendicular to the drift axis, extending from the ground surface down to the water table. The LDTH submodels include coupled TH processes and assume a heat-generation history that is effectively that of the entire waste-package inventory line-averaged over the total heated length of emplacement drifts in the repository. By interpolating three-dimensional SMT temperature results onto LDTH temperature results at different AML loadings, the *effective* AML is determined (5). This effective AML accounts for the influence of mountain-scale heat flow (including the edge-cooling effect) on local TH behavior and results in a *line-averaged TH* representation of the repository.

The influence of waste-package-to-waste-package deviations in local temperatures is addressed with the DDT submodels. The DDT submodels, which include the discrete waste packages, are run at the *modeled* AMLs. The DDT submodels represent thermal conduction in the emplacement drifts and host-rock, as well as thermal radiation between the surfaces of the open cavities in the emplacement drifts. Adding the waste-package-dependent temperature deviations calculated by DDT submodels onto the *line-averaged TH* predictions results in the final MSTHM output, which is equivalent to a Discrete-heat-source, Mountain-scale, ThermoHydrologic (DMTH) model, the final product of MSTHM (see (5) for details).

Recent Improvements to MSTHM

Recent improvements to the MSTHM include the ability to (1) represent a more complicated repository layout, (2) account for repository-scale thermal-conductivity K_{th} heterogeneity within the host-rock, and (3) address detailed pre-closure operational factors. Representing a more complicated repository layout is accomplished through the superposition of multiple SMT submodels. Repository-scale host-rock K_{th} heterogeneity is assembled from a series of realizations generated on the basis of laboratory measurements (14). The mean and standard-deviation of K_{th} are listed in Table I for each of the host-rock units; partially-saturated thermal conductivity are determined by linear interpolation between wet and dry values. Analyses of pre-closure operational factors are facilitated by a recently-developed capability to (1) predict TH conditions on a drift-by-drift basis for each 20-m interval along every emplacement drift, (2) represent sequential emplacement of waste packages along the drifts, (3) incorporate distance- and time-dependent heat-removal efficiency due to drift ventilation (done separately from MSTHM (15)), and (4) represent the influence of repository-scale K_{th} heterogeneity within each host-rock unit.

In a recent MSTHM analysis of a long-duration pre-closure ventilation case, a repository layout (16) with multiple non-parallel emplacement planes (Fig. 1) is accommodated using a superposition process that combines results from two SMT submodels (Fig. 2). This is justified by the linearity of the transient thermal conduction equation, which can accommodate K_{th} heterogeneity between and within the respective hydrostratigraphic units. The superposition process has been validated for several heterogeneous K_{th} realizations.
Each 20-m interval of every emplacement drift is discretely represented in the MSTHM output. Such detail accounts for the influence of sequential waste-package emplacement and distance- and time-dependent drift-ventilation heat-removal efficiency for all emplacement drifts throughout the repository. For the analysis of a long-duration pre-closure ventilation case, the local start of heating and the effective waste-age correspond exactly to waste-package-emplacement sequencing, a process occurring over a 52 year period (Fig. 3). The heat-removal efficiency of drift ventilation is treated as a function of time (beginning with the start of ventilation), and distance is measured from the ventilation inlet of the emplacement drift. Note that heat-removal efficiency, which is defined to be the percentage of the waste-package heat-output removed by the ventilation air, decreases with increasing distance from the inlet of an emplacement drift. Thus, the net effective heat output from

waste packages furthest removed from the inlet, i.e., immediately adjacent to the ventilation exhaust port, is greatest, while the net effective heat output from waste packages adjacent to the ventilation inlet is least. To accommodate the necessary operational details of the multi-panel repository, 156 LDTH/SDT-submodel locations are required for this particular MSTHM analysis (Fig. 4). This number of locations adequately captures the variability of infiltration flux and stratigraphy over the multi-panel repository. Three of the 156 locations are chosen for further discussion and are the circled locations ($P2E_{CENTER}$, $P4E_{CENTER}$, and $P4W_{EDGE}$) in Fig. 4.

MSTHM RESULTS FOR A LOWER TEMPERATURE REPOSITORY

To investigate the relative importance of addressing the sequential emplacement of waste packages in the MSTHM, two different cases are considered. In the *sequential-emplacement case*, waste packages are sequentially emplaced in the multiple repository panels. In the SMT submodel, this sequential heating is implemented as a smeared heat source block-by-block on a 20-m by 20-m basis along each of the emplacement drifts, with each 20-m interval having its own unique time of emplacement, the start-time for heating. In the drift-scale submodels, including the LDTH, SDT, and DDT submodels, the start-time of heating is equal to the start-time in the corresponding SMT-submodel grid block. In the *simultaneous-emplacement case*, waste packages are simultaneously emplaced in all MSTHM submodels at the midpoint (~26 years) of the 52 year emplacement period.

Recent improvements in accounting for sequential-loading are applied to the *sequential-emplacement case*. Waste packages are spaced apart an average of 2 m to yield a line-averaged thermal load of 1.15 kW/m of emplacement drift and are sequentially emplaced throughout the repository during the 52 year period. Forced ventilation of the drifts occurs from 98 years (for the last emplaced waste package) to 150 years (for the first emplaced waste package). The same generic heat-generation curves for each of the respective waste-package types are used throughout the repository, with the onset of heating corresponding to the local time of emplacement. For example, the first emplaced waste packages have heat-generation curves that are shifted by 0 years, while the last emplaced waste packages have curves that are shifted by 52 years.

The ability of the MSTHM to represent temperature conditions both within the emplacement drift and within the host-rock is demonstrated in Fig. 5 and Fig. 6, which show the *line-averaged temperatures* for a location close to the repository edge ($P4W_{EDGE}$) and a location close to the repository center ($P4E_{CENTER}$). At both locations, waste packages are emplaced towards the end of the emplacement period. A comparison of Fig. 5 and Fig. 6 clearly shows the influence of the edge-cooling effect. Note that the edge location (top plots) cools down more quickly than the center location (bottom plots). Also note that for the $P4E_{CENTER}$ location the radial extent of temperature increase in the host-rock is larger at 500 years than it is at 200 years even though the peak temperatures are lower, representing the thermal reinforcement, i.e., lack of edge-cooling, occurring at the repository center. Conversely, the radial extent of host-rock temperature increase is smaller at 500 years than it is for 200 years for the edge location. The corresponding *line-averaged hydrologic variable* of relative humidity (*RH*) is shown in Fig. 7 (*RH* at 200 years) and Fig. 8 (*RH* at 500 years). It is worth noting that for the edge location, the region of low *RH* is limited to the vicinity of the waste-package for the edge location while it extends out of the drift into the host-rock for the center location. Recall that MSTHM captures the discrete TH history in and near the drift for each waste package by incorporating DDT temperature histories onto the *line-*

averaged TH results. As an example of the temperature histories generated for each waste-package at a particular location, consider the center location ($P4E_{CENTER}$) as illustrated in Fig. 9. Here, the hottest package (PWR1-2) exceeds boiling briefly at about 200 years while a cooler package (BWR) peaks at 78^{o}C. It is worth noting the temperature differences modeled between the waste-package (T_{wp}), the drip-shield (T_{ds}) and the drift wall (T_{dw}) for the PWR packages are nearly as great as the temperature differences between hot and cold waste-packages.

Of particular importance in this modeling study is the ability to represent a complex repository layout, consisting of multiple panels (Fig. 1), as well as the ability to represent the sequential emplacement of waste packages. Prior to this study, all MSTHM analyses assumed a repository layout of a single contiguous panel with all waste packages simultaneously emplaced (1,2,3,4). To evaluate the relative importance of representing sequential emplacement, consider the temperature difference between a case assuming simultaneous waste-package emplacement and a case accounting for sequential waste package emplacement. Figures 10 and 11 illustrate comparisons of waste-package temperatures for *simultaneous-emplacement* versus *sequential-emplacement* at a repository location of early emplacement and at a repository location of late emplacement, respectively. The assumption of simultaneous emplacement results in higher peak temperatures than the sequential-emplacement case for locations of early-emplacement, because sequential-emplacement results in greater ventilation (150 years vs. 100 years) and, hence, a lower peak temperature (Fig. 10). Conversely, the assumption of simultaneous emplacement results in similar peak temperatures when compared to temperatures histories associated with locations of late-emplacement (Fig. 11). A similar temperature peak occurs because the ventilation period is the same for the simultaneous-loading as they are for late-emplacement locations. It is worth noting, however, temperatures drop off much more rapidly for the sequentially loaded packages of Fig. 11, thus capturing the edge-cooling effects of an overall cooler repository modeled by sequential emplacement.

For this *simultaneous-emplacement* case, greater-than-average heat-output waste packages generally result in above-boiling temperatures. For the *sequential-emplacement* case, greater-than-average heat-output waste packages, i.e., the PWR waste packages, generally result in above-boiling temperatures, particularly for waste packages emplaced towards the end of the emplacement period. Less-than-average heat-output waste packages, i.e., HLW and BWR waste packages, generally never result in above-boiling temperatures. It is important to note that the “hotter” nature of the simultaneously loaded repository is an artifact of our choosing the sudden-emplacement to occur with only 98 years of ventilation. Had we chosen a sudden-emplacement with 150 years of ventilation, the *simultaneous-emplacement* loaded repository would in fact be “cooler” than the *sequential-emplacement* repository. The comparison of simultaneous- versus sequential-emplacement illustrates the spatially variable nature of the peak-temperatures and cool-down periods for a case of prolonged (50+ years) waste-package loading of the repository.

MODELNG HOST-ROCK THERMAL CONDUCTIVITY HETEROGENEITY

A process for representing the influence of repository-scale K_{th} heterogeneity in the host-rock units is a recent developed for MSTHM and was tested on this lower temperature exercise. A total of 50 geostatistically varying realizations for repository-scale K_{th} heterogeneity were provided by BSC (15). The three parameters varied for these realizations were wet and dry thermal conductivity, and dry bulk density with a vertical length scale of

~2m and a horizontal length scale of ~50 m. It should be noted that the grid blocks representing the heated portions of the emplacement drifts in the SMT have horizontal dimensions of 20 m (along the drift axis) by 81 m (perpendicular to the drift axis). Because the heterogeneity horizontal length scale is roughly equal to the horizontal dimensions of the heated grid blocks for the SMT, and because the length scale is roughly equal to the horizontal dimensions of the LDTH/SDT/DDT submodel, K_{th} heterogeneity is incorporated in a "layer-cake" fashion for the drift-scale submodels. Repository-scale K_{th} heterogeneity is evaluated randomly about a normalized distribution and is addressed within each of the four primary host-rock units (see Fig. 12), including the Tptpul (Topopah Spring Upper Lithophysal unit, often referred to as "tsw33"), Tptpmn (Topopah Spring Middle Non-lithophysal unit, often referred to as "tsw34"), Tptpll (Topopah Spring Lower Lithophysal unit, often referred to as "tsw35"), and Tptpln (Topopah Spring Lower Nonlithophysal unit, often referred to as "tsw36"). The mean K_{th} and the standard deviation in K_{th} for each host-rock unit is listed in Table I. At the $P4E_{CENTER}$ location (see Figure 4), the MSTHM was used to analyze a set of 50 heterogeneous-K_{th} realizations.

Prior to conducting sensitivity analyses for this MSTHM effort, the inclusion of repository-scale heterogeneity for all combinations of submodels required testing. The possible combinations are the following: (1) inclusion in all submodels, (2) inclusion in SMT only, (3) inclusion in DDT only, and (4) inclusion in LDTH only. Only two of these combinations adequately represent the effect of repository-scale K_{th} heterogeneity: (1) a "comprehensive" approach that incorporates the repository-scale K_{th} heterogeneity in all four of the MSTHM submodels (LDTH, SMT, SDT, and DDT), and (2) a "LDTH-only" approach that incorporates the repository-scale K_{th} heterogeneity in only LDTH submodels.

Two waste-package temperature histories (PWR1-2 and DHLW) for the $P4E_{CENTER}$ location are compared for two different approaches of representing repository-scale K_{th} heterogeneity (Fig. 13). Representing K_{th} heterogeneity in all submodels does not affect peak temperatures, however, it has a small but noticeable effect on temperatures during the 500 to 2000 year timeframe. The primary purpose of the SMT submodels is to determine the rate at which the "edge-cooling" effect influences local temperatures. At the $P4E_{CENTER}$ location, the edge-cooling effect requires several hundred years to be manifested. Consequently, the small influence of repository-scale K_{th} heterogeneity in the SMT/DDT/SDT submodels is not notable until about 500 years. Because the evolution of the edge-cooling effect is weakly affected by repository-scale K_{th} heterogeneity, it is not necessary to include K_{th} heterogeneity in the SMT submodels. For the type of heterogeneity illustrated here, simulations indicate that it may only be necessary to represent repository-scale K_{th} heterogeneity in the LDTH submodels.

A set of 50 realizations randomly varying thermal conductivity (K_{th}) in the manner described above is run to demonstrate the overall effect of K_{th} heterogeneity. For these realizations, K_{th} heterogeneity is represented only in the LDTH submodels, and the variation in waste-package temperature for the 50 realizations at location $P4E_{CENTER}$ is illustrated in Fig. 14 for the hottest package, PWR1-2, and in Fig. 15 for the coolest package, DHLW. The maximum range in waste-package temperatures is about 11.5^{o}C at a time of 180 yr for these 50 realizations. The effect on the temperature history of thermal-conductivity heterogeneity is small for the sub-boiling design addressed in this study: the temperature deviation for 50 realizations with geostatistically varied K_{th} is almost half the temperature deviation simulated between hot and cold waste-packages, which is about 20^{o}C at 180 years (see Fig. 9). It is anticipated that the temperature variation due to thermal conductivity variation will be larger for an above-boiling design.

CONCLUSIONS

The modeling effort discussed represents an early investigation of a nuclear waste repository simulated at a lower temperature mode. It needs to be noted that these simulations have a different panel loading than the repository currently being considered for license application at Yucca Mountain. This exercise allowed further enhancement of the MultiScale ThermoHydrologic Model (MSTHM) to accommodate a complex repository layout with emplacement drifts lying in non-parallel planes through the superposition of multiple mountain-scale submodels. A second improvement made during this exercise was the incorporation of thermal-conductivity heterogeneity within each host-rock type, while a third improvement was the incorporation of detailed pre-closure operational factors including the ability to (1) predict TH conditions on a drift-by-drift basis, (2) to represent sequential emplacement of waste packages along the drifts, and (3) to incorporate the distance- and time-dependent heat-removal efficiency associated with pre-closure drift ventilation.

The differences in MSTHM output that occur when implementing these new capabilities were demonstrated with a new sequential waste-package loading simulation compared to a standard simultaneous loading simulation. The new simulations anticipate, as before, the sharp temperature rise and drift dry-out followed by a long cool-down and re-wetting period. Peak temperature differences within the drift were ~20^{o}C, similar in magnitude to differences between peak waste-package temperatures of hotter and cooler packages. Depending on the emplacement-period duration, emplacement sequencing can influence local thermohydrologic conditions. For the relatively long emplacement period considered in this study (52 years), it is important to address emplacement sequencing, as the temperature peaks are different at some locations and the "edge-cooling" effects on the sequentially loaded drifts results in modified cool-down histories. It needs to be noted, however, that for shorter emplacement periods (less than 25 years), the differences between instantaneous and sequential emplacement are less significant.

Alternative approaches were investigated during this study to address repository-scale thermal-conductivity (K_{th}) heterogeneity in the host-rock. Geostatistically varied K_{th} values with a horizontal length scale of 50m and a vertical length scale of 2m were used to approximate heterogeneity within each host-rock unit. From MSTHM realizations based on these values, it is concluded that MSTHM can adequately represent temperature variations due to repository-scale thermal-conductivity heterogeneity by propagating heterogeneity in only the LDTH submodel. Such a simplification greatly assists in MSTHM analysis incorporation of parameter variation. Propagating a range of parameter values only through the LDTH submodels will enable the MSTHM to efficiently address heterogeneity and uncertainty of other parameters, e.g., percolation flux and permeability. A total of 50 MSTHM realizations of geostatistically varied host-rock thermal conductivity were run to determine the overall effect of host-rock K_{th} variability. The effect on the temperature history of thermal-conductivity heterogeneity is small for the sub-boiling design addressed in this study being almost half the temperature deviation simulated between hot and cold waste-packages. Temperature variation due to thermal conductivity variation will be larger for an above-boiling design.

ACKNOWLEDGEMENTS

This work was supported is supported by the Yucca Mountain Project. This work was performed under the auspices of the U.S. Department of Energy by University of California Lawrence Livermore National Laboratory under contract No. W-7405-Eng-48.

REFERENCES

(1) BSC (Bechtel SAIC Company), "Multiscale Thermohydrologic Model Report", ANL-EBS-MD-000049 REV 01, Las Vegas, NV (2003).

(2) BSC (Bechtel SAIC Company), "FY01 Supplemental Science and Performance Analyses, Vol. 1: Scientific Basis and Analyses", Rep. TDR-MGR-MD-000007 REV00 ICN01, Las Vegas, NV (2001).

(3) Civilian Radioactive Waste Management System (CRWMS), "Thermohydrologic Calculations for Site Recommendation/ License Application Design Selection, Phase 2", B0000000-01717-0210-00009 REV 00, Las Vegas, NV (1999).

(4) Civilian Radioactive Waste Management System (CRWMS), "Total System Performance Assessment–Site Recommendation Methods and Assumptions", TDR-MGR-MD-000001 REV 00, Las Vegas, NV (1999).

(5) T. A. Buscheck., L. G. Glascoe, K. H. Lee, J. Gansemer, Y. Sun and K. Mansoor, "Validation of the multiscale thermohydrologic model used for analysis of a repository at Yucca Mountain", *Journal of Contaminant Hydrology*, 62-63:421-440 (2003).

(6) T. A. Buscheck, N. D. Rosenberg, J. Gansemer and Y. Sun, "Thermohydrologic behavior at an underground nuclear waste repository at Yucca Mountain", NV. *Water Resources Research* 38(3), 10-1 – 10-19 (2002)

(7) T. A. Buscheck, N. D. Rosenberg, J. Gansemer, and Y. Sun, "Analysis of thermohydrologic behavior for above-boiling and below-boiling thermal-operating modes for a repository at Yucca Mountain", *Journal of Contaminant Hydrology*, 62-63:441-457 (2003).

(8) Y. S. Wu, C. Haukwa and G. S. Bodvarsson, "A site-scale model for fluid and heat flow in the unsaturated zone of Yucca Mountain", *Journal of Contaminant Hydrology*, 38:185-215 (1999).

(9) H. H. Liu, C. Doughty and G. S. Bodvarsson, "An active fracture model for unsaturated flow and transport in fractured rock", *Water Resources Research*, 34(10):2633-2646 (1998).

(10) R.W. Zimmerman, G. Chen, T. Hadgu and G. S. Bodvarsson, "A numerical dual-porosity model with semi-analytical treatment of fracture/matrix flow", *Water Resources Research*, 29(7):2127-2137 (1993).

(11) T. A. Busheck and J. J. Nitao. "The Impact of Buoyant, Gas-Phase Flow and Heterogeneity on Thermo-Hydrologic Behavior at Yucca Mountain", Lawrence Livermore National Laboratory, UCRL-JC-115351 (1994).

(12) J. J. Nitao, "Reference Manual for the NUFT Flow and Transport Code, Version 2.0", UCRL-MA-130651. Lawrence Livermore National Laboratory (1998).

(13) D. S. Rhoades and S. Brocoum, "Yucca Mountain site characterization project requirements document (YMP-RD)", YMP/CM-0025, REVISION 4, DCN 02 (2001).

(14) BSC (Bechtel SAIC Company), **“**Thermal Conductivity of the Potential Repository Horizon Model Report”, MDL-NBS-GS-000005 REV 00, Las Vegas (2002).

(15) BSC (Bechtel SAIC Company), “Ventilation Model”, ANL-EBS-MD-000030 REV 01 ICN 01, Las Vegas (2002).

(16) BSC (Bechtel SAIC Company), “Repository/PA IED Subsurface Facilities”, Document DWG-MGR-MD-000003-A. MOL.20020601.0194, Las Vegas (2002).

Table I. The wet and dry thermal-conductivity values used in the host-rock thermal-conductivity uncertainty study are summarized with mean and standard deviation. These data were obtained from BSC (14).

Host-rock unit	Dry thermal conductivity ($W/m^2\ {}^oC$)		Wet thermal conductivity ($W/m^2\ {}^oC$)	
	Mean	Std dev.	Mean	Std dev.
Tptpul (tsw33)	1.24	0.26	1.79	0.25
Tptpmn (tsw34)	1.42	0.27	2.07	0.25
Tptpll (tsw35)	1.28	0.25	1.89	0.25
Tptpln (tsw36)	1.49	0.28	2.13	0.27

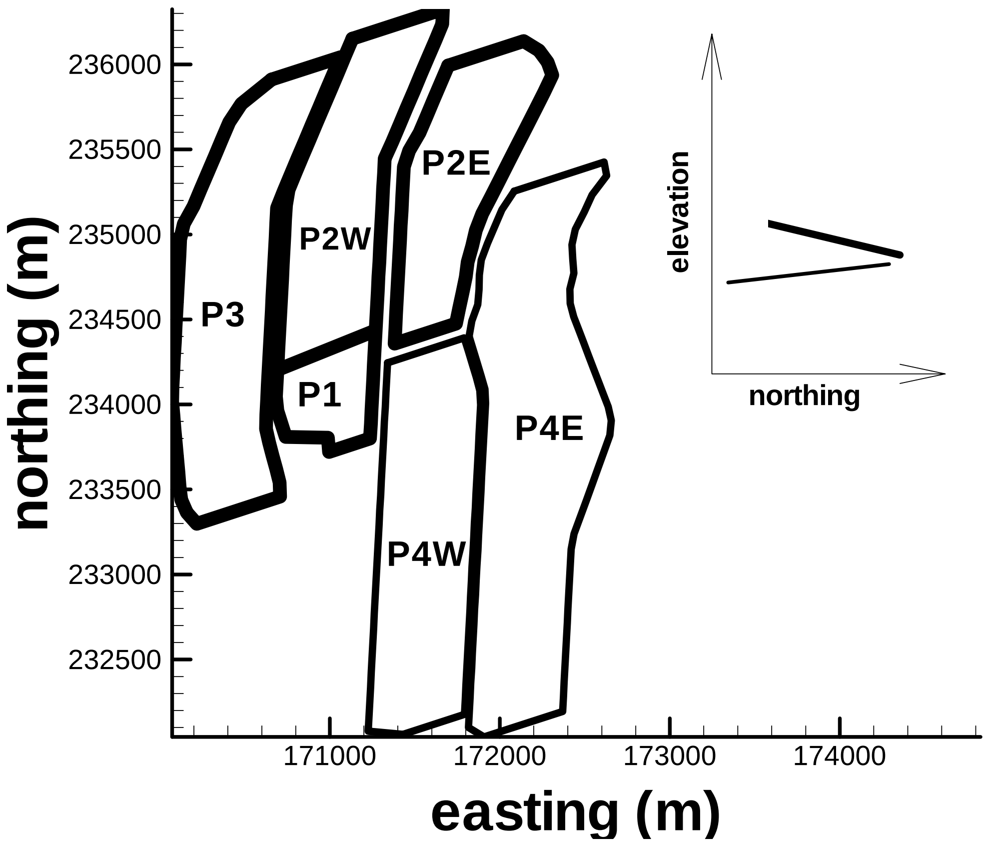

Figure 1. The repository layout considered in a recent MSTHM study in Nevada Coordinates [16]. This layout includes non-parallel emplacement planes labeled as: P1, P2E, P2W, P3, P4E, and P4W. Western panels P1, P2E, and P2W lie in one plane (see inset's heavy sloping line). Eastern panels P4E and P4W lie in a second plane (see the inset's lighter sloping line). Note that an additional panel (P5) south of P3 was considered a 'contingency' panel for this modeling exercise and, therefore, not included in this analysis.

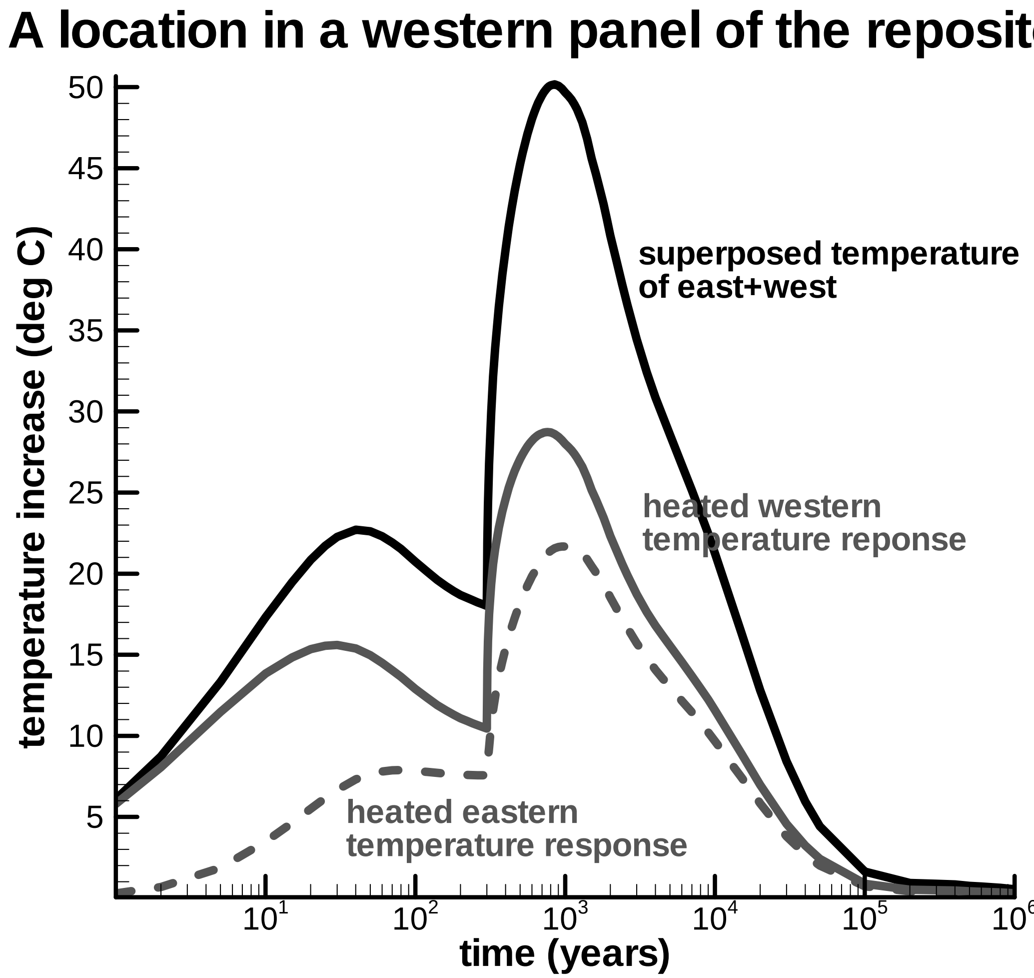

Figure 2. The superposition process combines the results from multiple SMT submodels. Computational demands of representing the complex 3-D details of the layout of the emplacement drifts and multiple panels can be distributed to multiple SMT submodels.

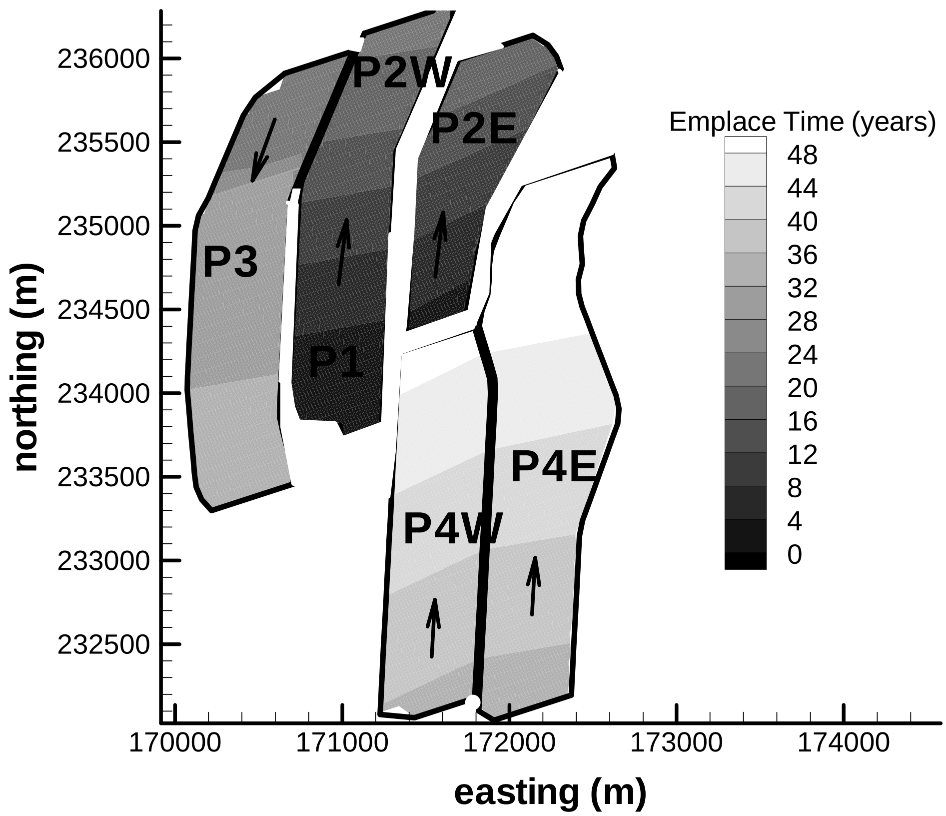

Figure 3. The simulations in this study address a repository in which waste packages are emplaced sequentially over a 52 year period.

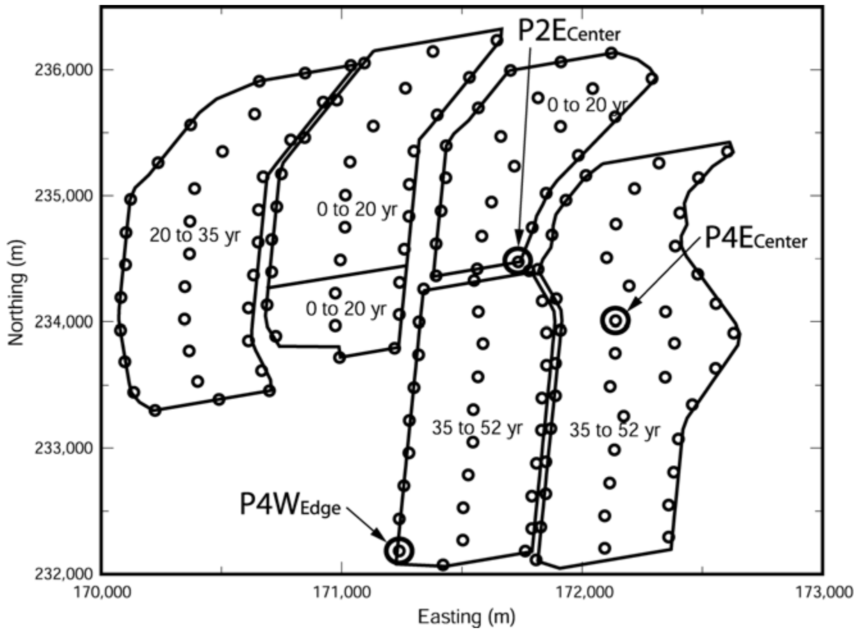

Figure 4. A total of 156 LDTH and SDT submodel locations are available for this analysis. The loading time, e.g., ‘20 to 35 yr’, of each panel is indicated. For this paper, the circled locations are discussed ($P2E_{CENTER}$, an early-loaded location; $P4E_{CENTER}$, a late-loaded center location; and $P4W_{EDGE}$, a late-loaded edge location).

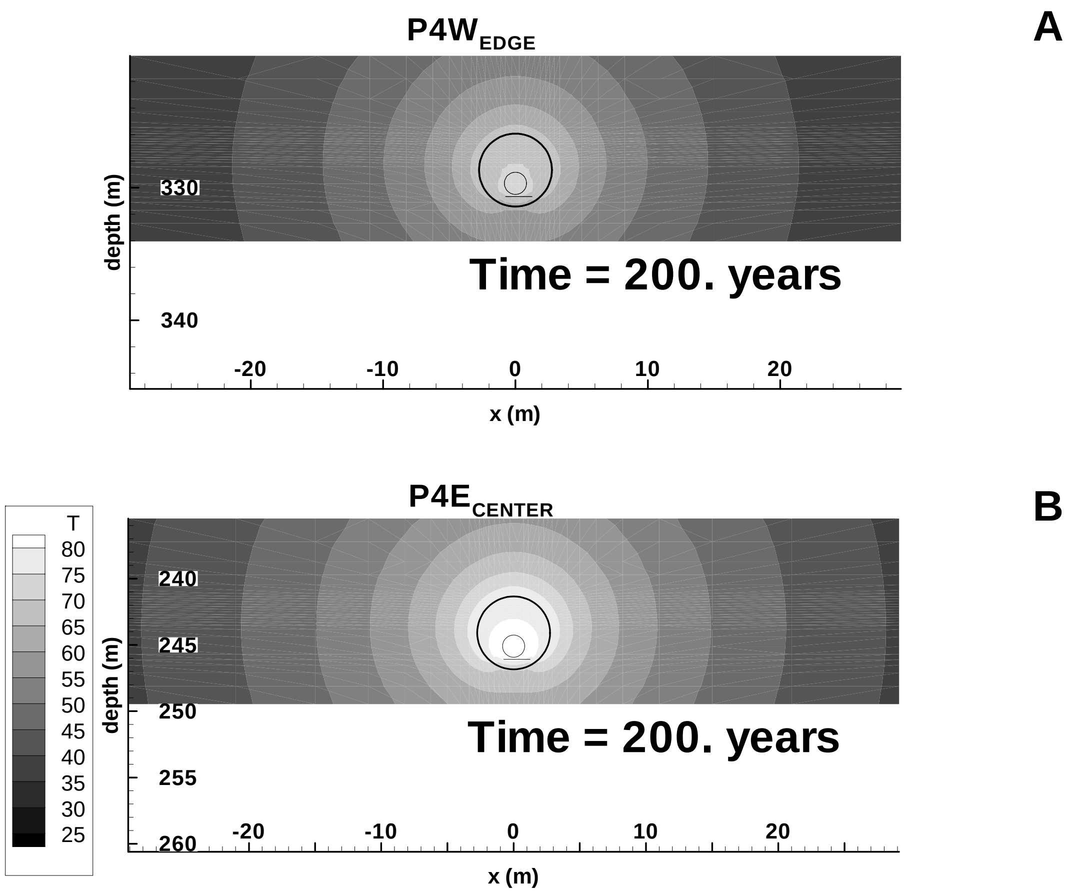

Figure 5. A vertical cross section of *line-averaged temperatures* with x=0 at the drift center and depth from surface. Plot A: at 200 yr for the $P4E_{EDGE}$ location, which is near the repository edge and where waste packages are emplaced towards the end of the emplacement period. Plot B: at 200 yr for the $P4E_{CENTER}$ location, which is near the center of the repository and where waste packages are emplaced towards the end of the emplacement period.

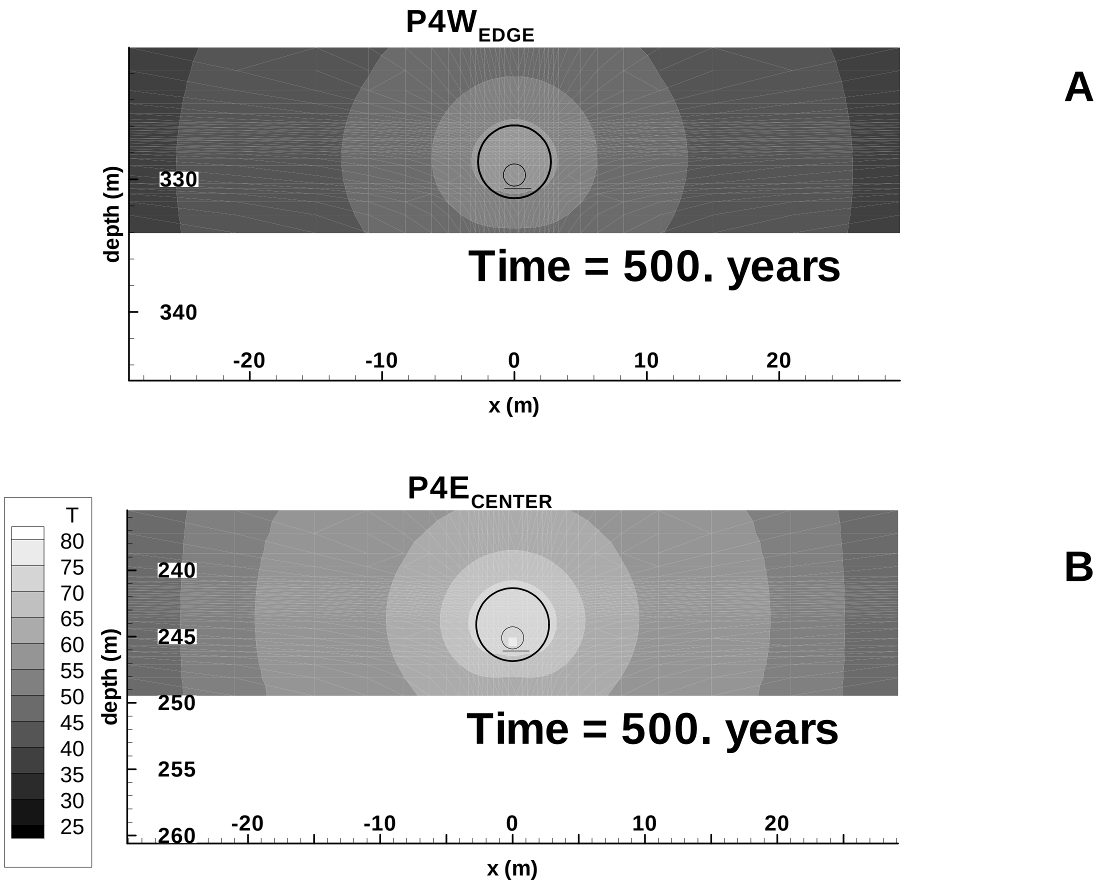

Figure 6. A vertical cross section of *line-averaged temperatures* with x=0 at the drift center and depth from surface. Plot A: at 500 yr for the $P4W_{EDGE}$ location, which is near the repository edge and where waste packages are emplaced towards the end of the emplacement period. Plot B: at 500 yr for the $P4E_{CENTER}$ location, which is near the center of the repository and where waste packages are emplaced towards the end of the emplacement period.

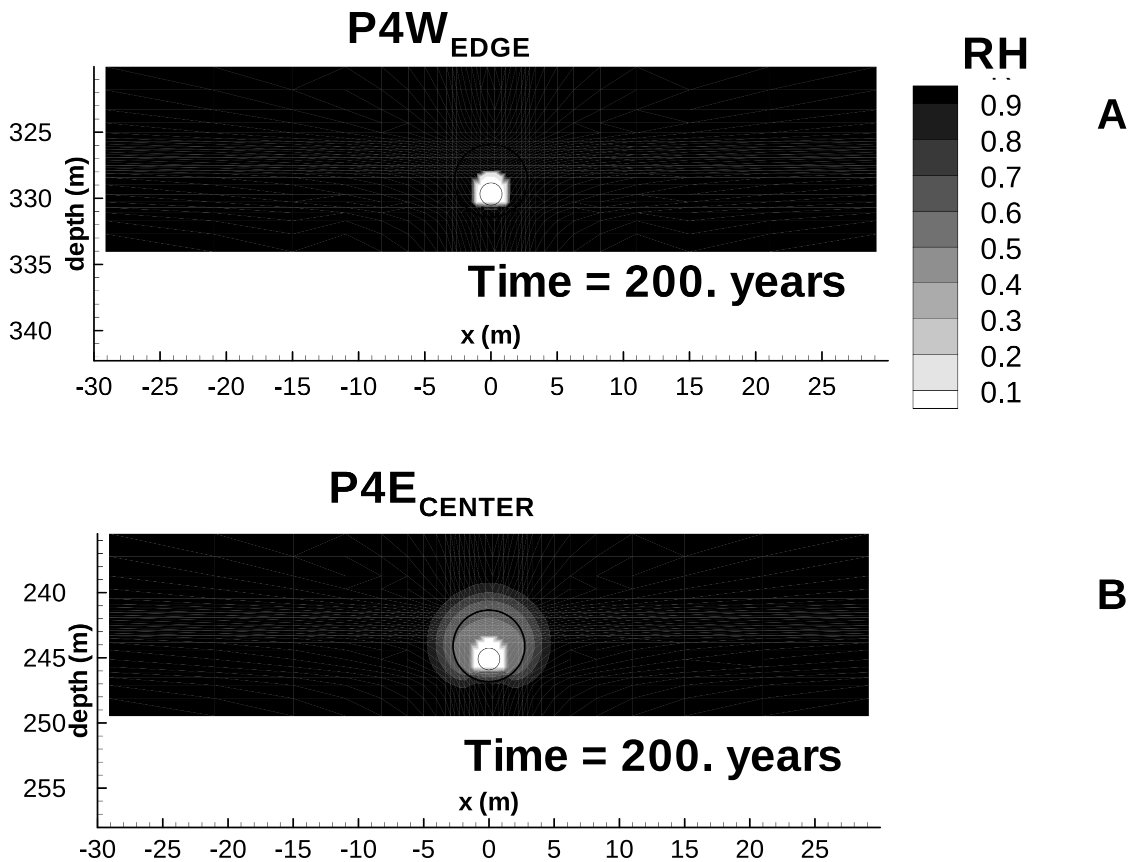

Figure 7. A vertical cross section of *line-averaged relative humidity* with x=0 at the drift center and depth from surface. Plot A: at 200 yr for the P4E$_{EDGE}$ location, which is near the repository edge and where waste packages are emplaced towards the end of the emplacement period. Plot B: at 200 yr for the P4E$_{CENTER}$ location, which is near the center of the repository and where waste packages are emplaced towards the end of the emplacement period.

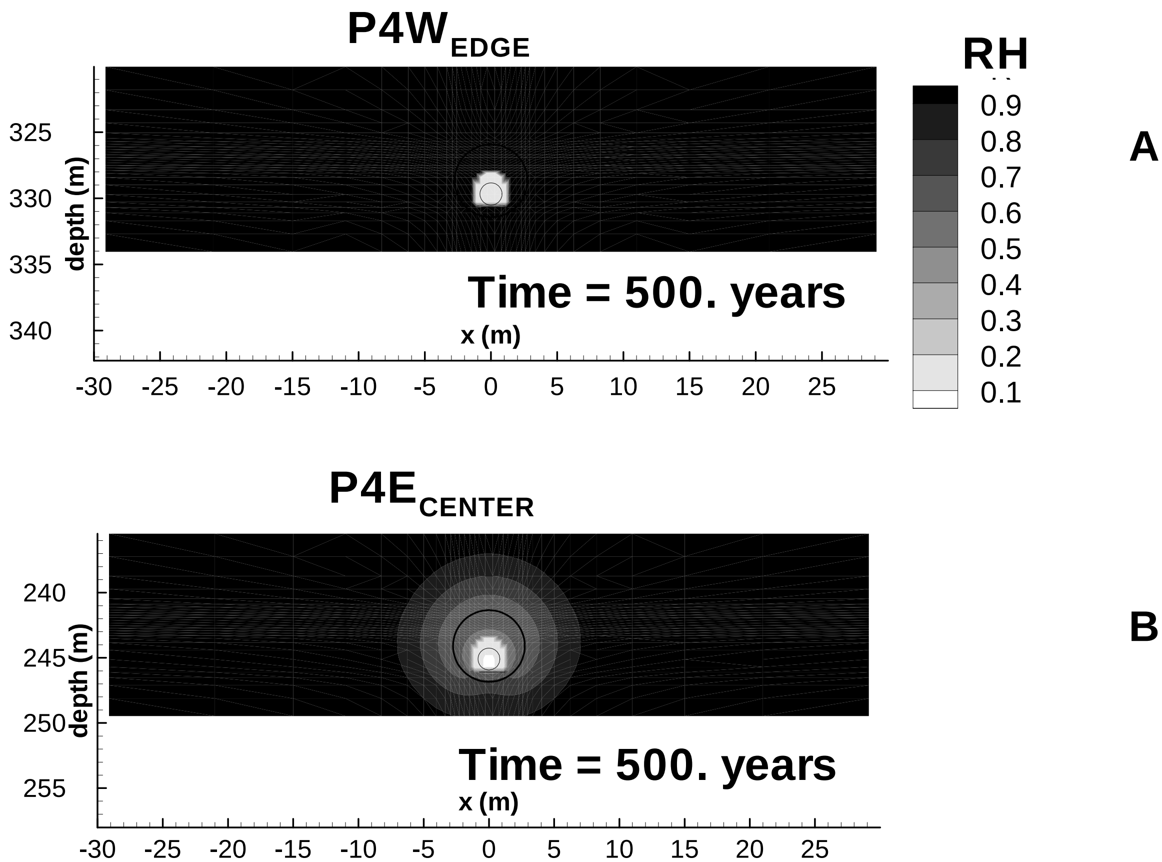

Figure 8. A vertical cross section of *line-averaged relative humidity* with x=0 at the drift center and depth from surface. Plot A: at 500 yr for the P4E$_{EDGE}$ location, which is near the repository edge and where waste packages are emplaced towards the end of the emplacement period. Plot B: at 500 yr for the P4E$_{CENTER}$ location, which is near the center of the repository and where waste packages are emplaced towards the end of the emplacement period.

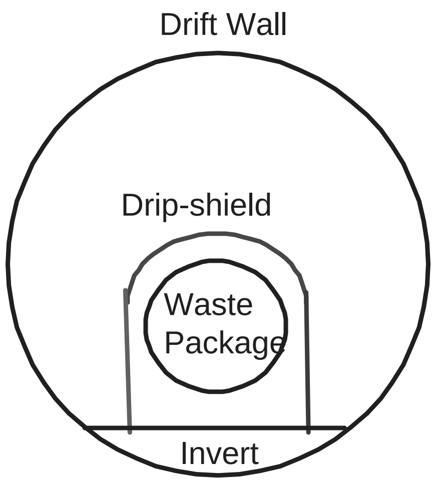

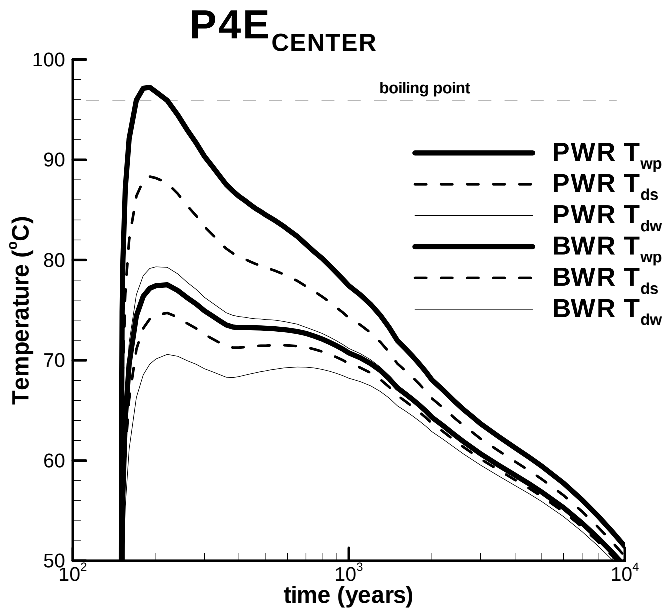

Figure 9. A conceptual model of the in-drift environment with hostrock (drift wall), drip-shield, and waste-package (LEFT PLOT). Discrete temperature histories at a location of early emplacement are shown for the waste-package (T_{wp}), on the drip-shield (T_{ds}), and on the drift-wall (T_{dw}) for the relatively hot PWR and relatively cool BWR waste packages (RIGHT PLOT).

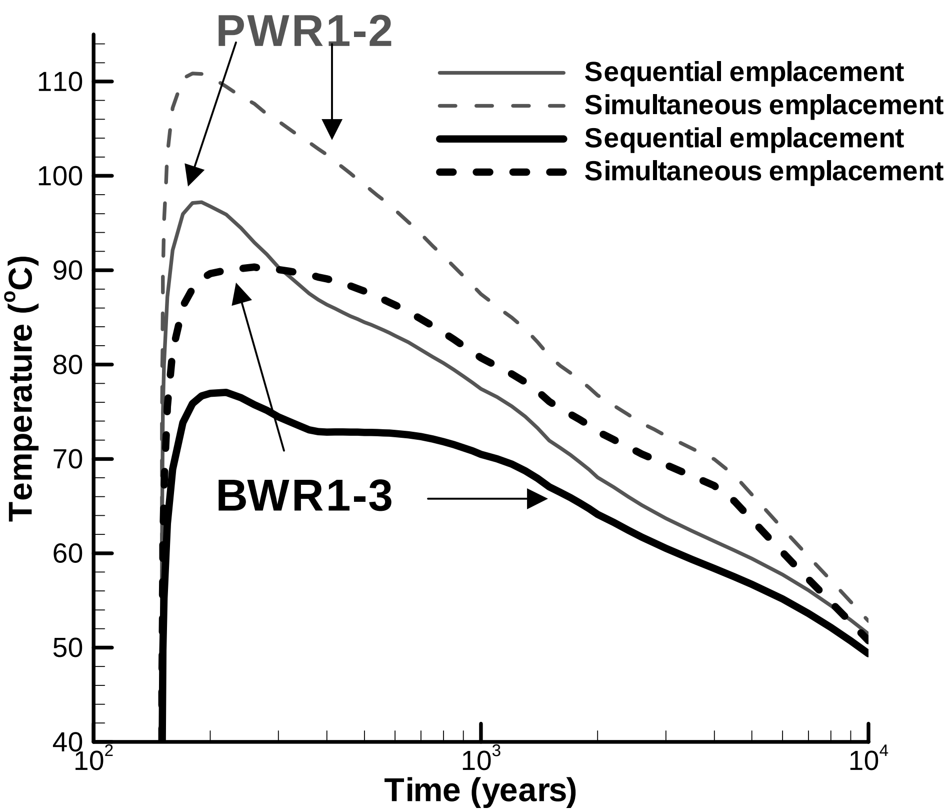

Figure 10. Discrete waste-package temperature histories are given for a PWR and a BWR waste package at a location emplaced during the early portion of the emplacement period ($P2E_{CENTER}$). The case that assumes simultaneous emplacement of waste results in higher peak temperatures than a case accounting for sequential emplacement.

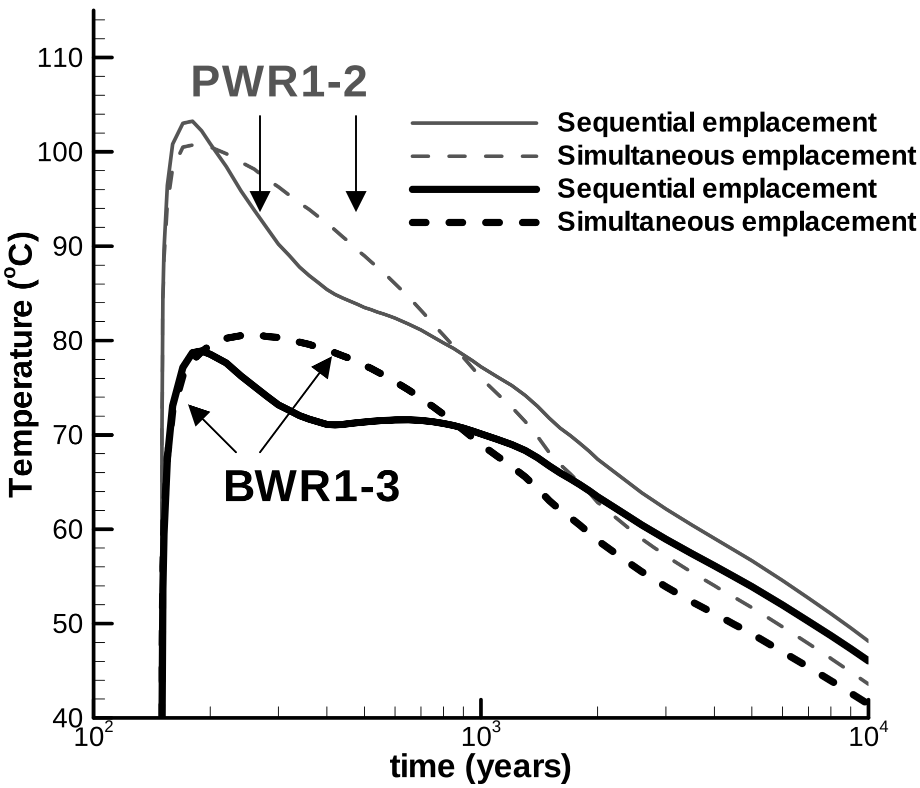

Figure 11. Discrete waste-package temperature histories are given for a PWR and a BWR waste package at a location emplaced during the latter portion of the emplacement period ($P4E_{CENTER}$). The case that assumes simultaneous emplacement of waste results in slightly lower peak temperatures than those predicted for the case accounting for sequential emplacement.

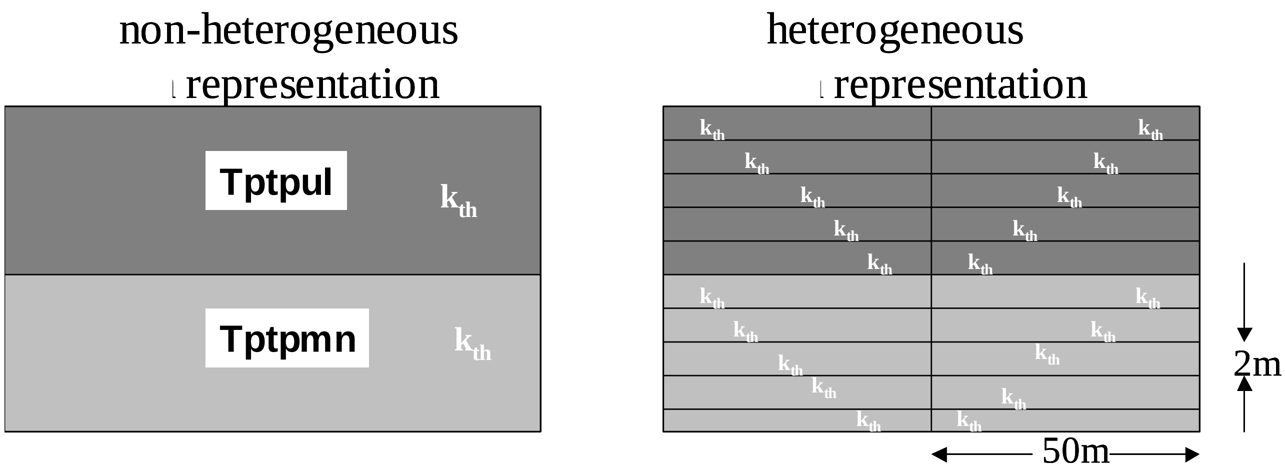

Figure 12. Repository-scale thermal conductivity (K_{th}) heterogeneity evaluated with normalized geostatistical variation about an average K_{th}. A total of 50 total realizations are considered, varying K_{th} at a horizontal and vertical length scales of ~50 m and ~2 m, respectively. Parameters varied were $K_{th,dry}$, $K_{th,wet}$, and ρ_b. Thermal conductivity (K_{th}) heterogeneity is modeled within each of four primary host-rock units: Tptpul, Tptpmn, Tptpll, and Tptpln.

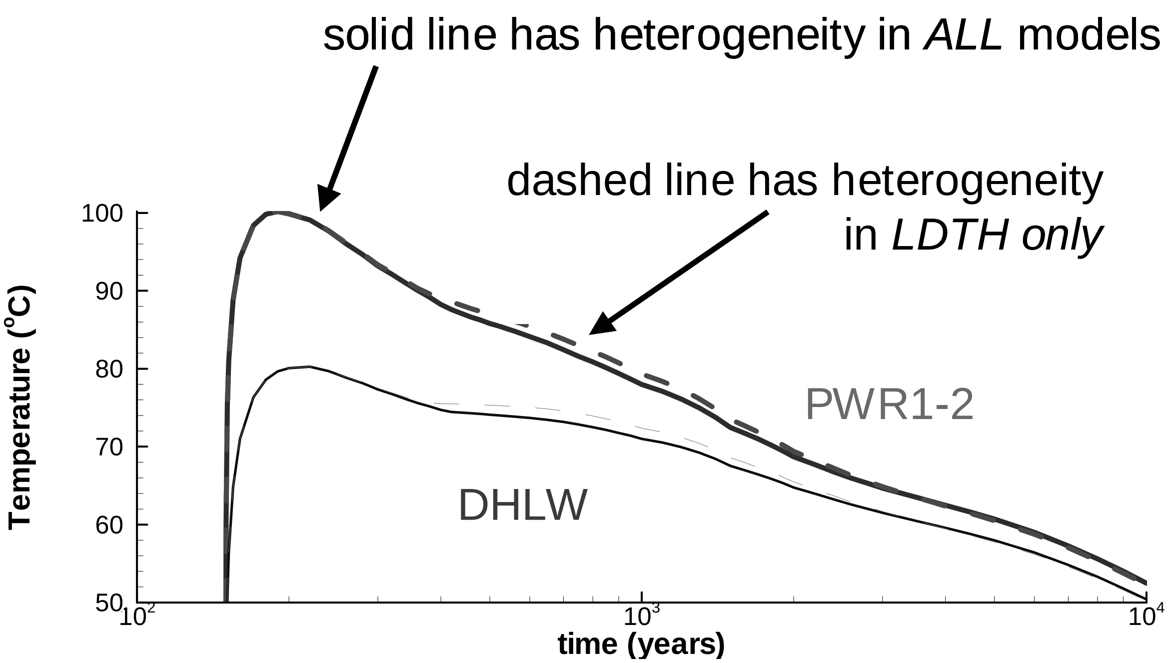

Figure 13. Discrete waste-package temperature histories (PWR1-2, heavy higher-temperature lines; and DHLW, light lower-temperature lines) for the P4E$_{CENTER}$ location are compared for different approaches to representing repository-scale K_{th} heterogeneity: with all submodels (solid lines), and with only LDTH submodels (dashed lines).

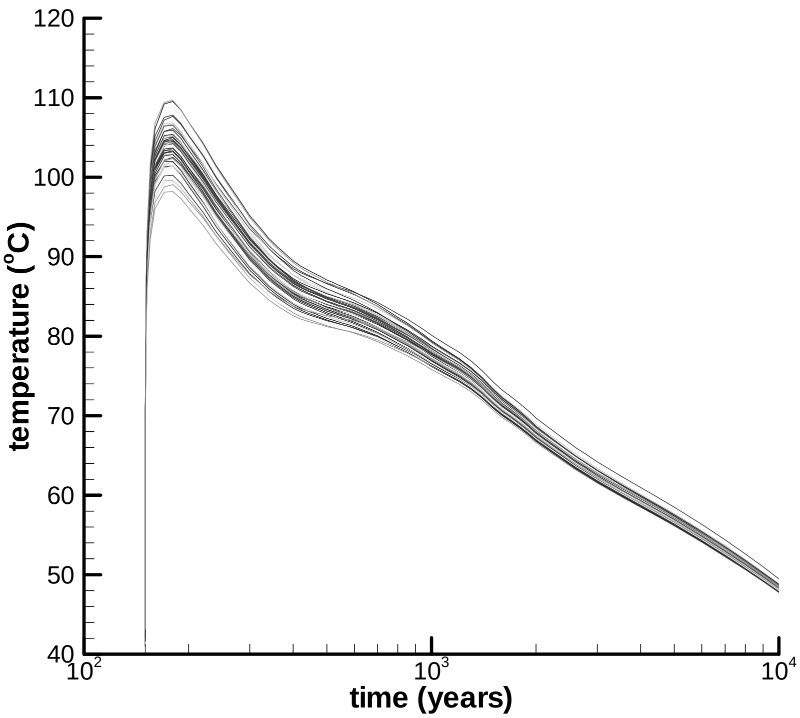

Figure 14. Discrete PWR1-2 waste-package temperature histories of all 50 repository-scale heterogeneous K_{th} realizations at location $P4E_{CENTER}$. At 180 years a maximum temperature difference of 11.4°C occurs for the PWR1-2 waste package, the package of greatest heat output.

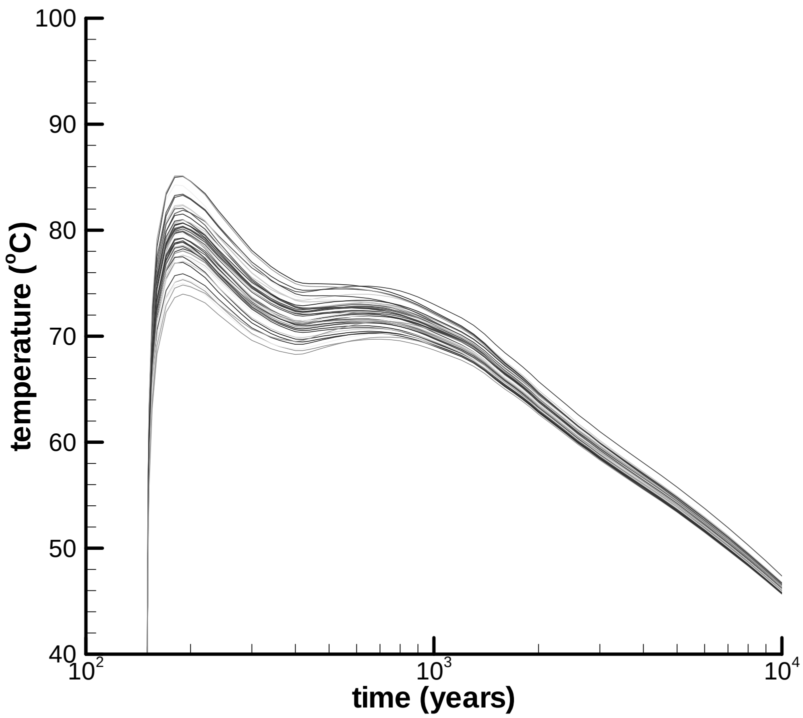

Figure 15. Discrete DHLW waste-package temperature histories of all 50 repository-scale heterogeneous K_{th} realizations at location P4E$_{CENTER}$. At 180 years a maximum temperature difference of 11.4°C occurs for the DHLW waste package, the package of lowest heat output.